Supporting information

Controllable synthesis of a non-interpenetrating microporous metal–organic framework based on octahedral cage-like building units for highly efficient reversible adsorption of iodine

Wen-Wen He, Shun-Li Li, Guang-Sheng Yang, Ya-Qian Lan*, Zhong-Min Su* and Qiang Fu

Institute of Functional Material Chemistry; Faculty of Chemistry, Northeast Normal University, Changchun, 130024, People's Republic of China; E-mail: lanyq176@nenu.edu.cn; zmsu@nenu.edu.cn

S1. Materials and measurements

All chemical materials were purchased from commercial sources and used without further purification. The FT-IR spectra were recorded from KBr pellets in the range 4000–400 cm^{-1} on a Mattson Alpha-Centauri spectrometer. The phase purities of the bulk samples were identified by X-ray powder diffraction on a Rigaku, Rint 2000 diffractometer. The UV-Vis absorption spectra were examined on a Shimadzu UV-2550 spectrophotometer in the wavelength range of 200-800 nm. The C, H, and N elemental analyses were conducted on a Perkin-Elmer 240C elemental analyzer. TGA was performed on a Perkin–Elmer TG-7 analyzer heated from room temperature to 1000 ºC at a ramp rate of 5 °C/min under nitrogen. The photoluminescence spectra were measured on a Perkin-Elmer FLS-920 Edinburgh Fluorescence Spectrometer. ICP was measured by ICP-9000 (N+M) (USA Thermo Jarrell-Ash Corp). Electrical measurements (Keithley Source metre 2400) on single crystals were performed by contacting them with Au paste. The N_2 sorption measurements were performed on an automatic volumetric adsorption equipment (Belsorp mini II). Before gas adsorption measurements, the sample was immersed in methanol for 24 h, and the extract was decanted. Fresh methanol was subsequently added, and the crystals were allowed to stay for an additional 24 h to remove the nonvolatile solvates. The sample was collected by decanting and treated with dichloromethane similarly to remove methanol solvates. After the removal of dichloromethane by decanting, the sample was activated by drying under a dynamic vacuum at room temperature overnight. Before the measurement, the sample was dried again by using the ‘outgas’ function of the surface area analyzer for 12 h at room temperature.

S2. Synthesis of IFMC-15

$Zn(NO_3)_2 \cdot 6H_2O$ (0.078 g, 0.262 mmol), H_3BPTC (0.020 g, 0.070 mmol), H_2BDC (0.003 g, 0.017 mmol) were dissolved in 10 ml DMF, and then 3 drops of HBF_4 were added. The mixture was placed in a Teflon reactor and heated at 110 °C for 3 days, and then it was gradually cooled to room temperature. The crystals were obtained in a 58% yield. Elemental microanalysis for $[NH_2(CH_3)_2] \cdot [Zn_4O(BPTC)_2(BDC)_{0.5}] \cdot 8DMF$, calculated (%): C, 46.33; H, 5.15; N, 8.11. Found (%): C, 45.47; H, 4.90; N, 7.86. IR (cm^{-1}): 3730.02 (w), 3436.75 (s), 2928.93 (w), 1658.57 (s), 1393.06 (s), 1096.96 (m), 772.59 (m), 722.57 (m), 662.39 (w).

S3. X-ray crystallography

Single-crystal X-ray diffraction data for **IFMC-15** was recorded by using a Bruker Apex CCD diffractometer with graphite-monochromated Mo-Kα radiation (λ = 0.71069 Å) at 293 K. Absorption corrections were applied by using a multi-scan technique. All the structures were solved by Direct Method of SHELXS-97 and refined by full-matrix least-squares techniques using the SHELXL-97 program within WINGX. Non-hydrogen atoms were refined with anisotropic temperature parameters. The SQUEEZE program implemented in PLATON was used to remove these electron densities for **IFMC-15**. Thus, all of electron densities from free solvent molecules have been "squeezed" out.

The detailed crystallographic data and structure refinement parameters for **IFMC-15** are summarized in Table S1.

Table S1 Crystal data and structure refinements for compound **IFMC-15**.

Identification code	**IFMC-15**
formula	$C_{60}H_{80}N_9O_{23}Zn_4$
Formula weight	1556.81
Crystal system	Monoclinic
Space group	$P2_1/c$
a (Å)	10.2830(11)
b (Å)	27.339(3)
c (Å)	28.6471(16)
α (°)	90.00
β (°)	108.204(3)
γ (°)	90.00
V (Å^3)	7648.4(12)
Z	4
$D_{calcd.}$[g cm^{-3}]	1.352
F(000)	3228
Reflections collected	38450 / 13550
R(int)	0.0869
Goodness-of-fit on F^2	0.922
$R_1{}^a$ [I>2σ (I)]	0.0407
$wR_2{}^b$	0.0503

$^aR_1 = \Sigma||F_o|-|F_c||/\Sigma|F_o|$. $^bwR_2 = |\Sigma w(|F_o|^2-|F_c|^2)|/\Sigma|w(F_o^2)^2|^{1/2}$.

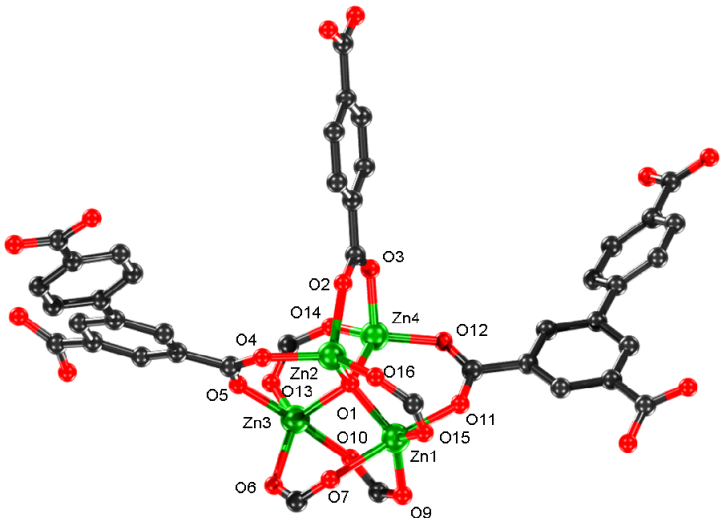

Fig. S1 The coordination environment of Zn in **IFMC-15**.

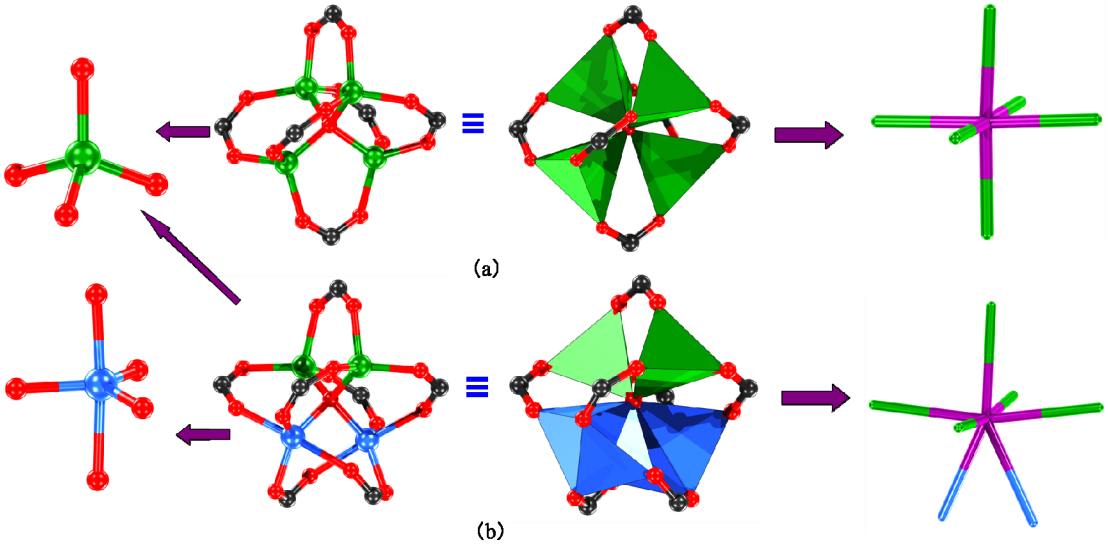

Fig. S2 Two kinds of Zn_4O SBU, $Zn_4O(CO_2)_6$ SBU in **IRMOF-n** (a) and $Zn_4O(CO_2)_7$ SBU in **IFMC-15** (b).

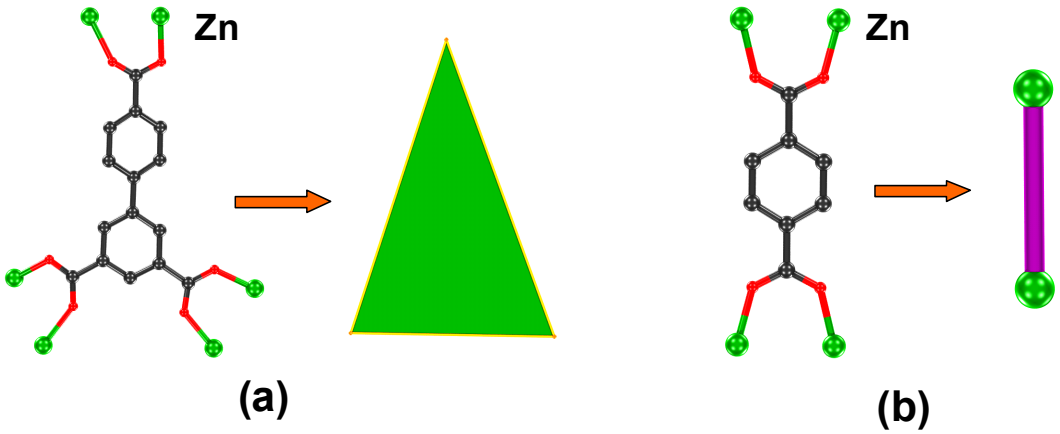

Fig. S3 The coordination modes of ligands in **IFMC-15**.

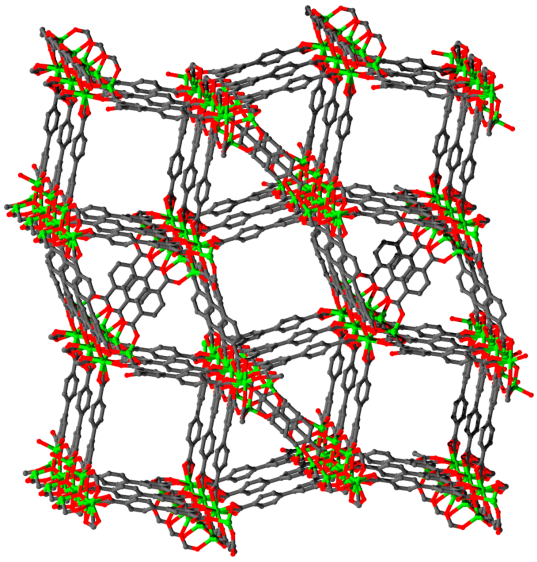

Fig. S4 Ball-and-stick representations of the 3D structure of **IFMC-15**.

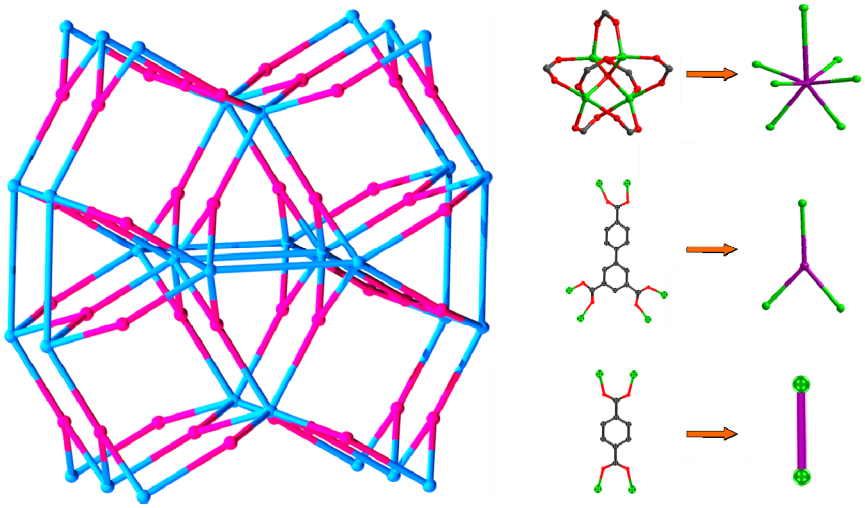

Fig. S5 The (3, 7)-connected topology network in **IFMC-15**.

Topological analysis for **IFMC-15** by OLEX.

Topological Terms for	short[a]	long[b]
three-connected node	4.5(2)	4.5.5
seven-connected node	4(2).5(5).6(10).8(4)	4.4.5.5.5.5(2).5.6.6.6.6.6.6.6.6(2).6(2).6

[a]The short Schläfli symbol is $(4\cdot5^2)_2\cdot(4^2\cdot5^5\cdot6^{10}\cdot8^4)$;

[b]The long Schläfli symbol is $(4\cdot5\cdot5)_2\cdot(4\cdot4\cdot5\cdot5\cdot5\cdot5_2\cdot5\cdot6\cdot6\cdot6\cdot6\cdot6\cdot6\cdot6\cdot6_2\cdot6_2\cdot6)$.

Topological analysis by OLEX reveals that **IFMC-15** can be defined as a 3D (3, 7)-connected network, in which the $BPTC^{3-}$ ligand is regarded as a three-connected node, the BDC^{2-} ligand is regarded as a linker of two $[Zn_4O(CO_2)_7]$ SBUs and the $[Zn_4O(CO_2)_7]$ SBU is regarded as a seven-connected node.

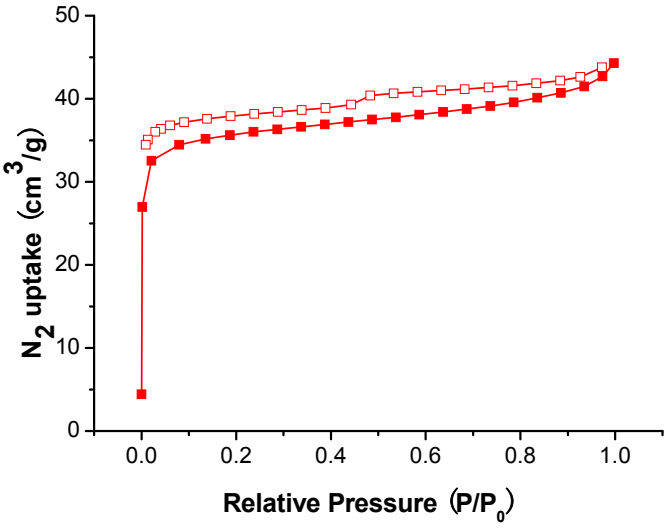

(a)

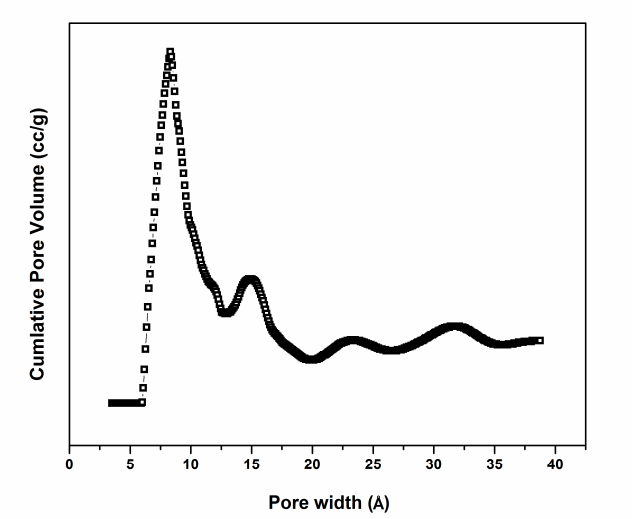

(b)

Fig. S6 (a) The N_2 gas-sorption isotherms for **IFMC-15** measured at 77 K, 1 atm (BET surface area: 138 m^2/g; Langmuir surface area: 158 m^2/g). The filled and open squares represent adsorption and desorption branches, respectively. (b) The pore size distribution of **IFMC-15** (analysis by SF method).

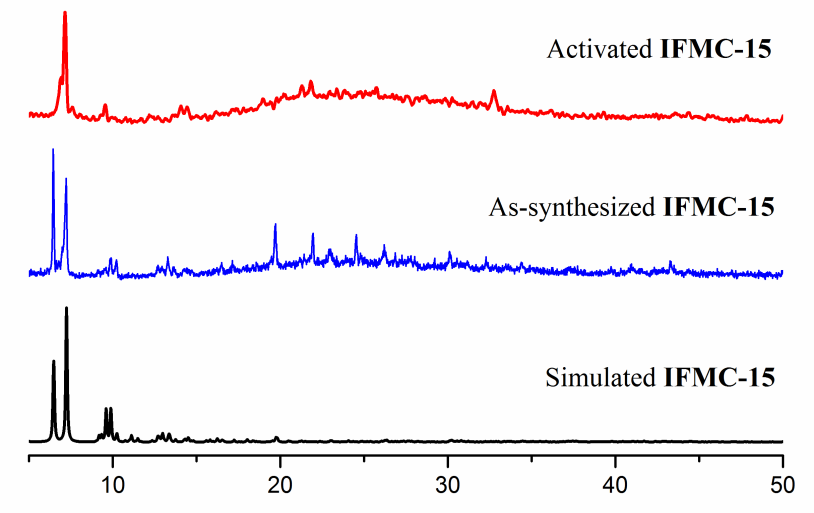

Fig. S7 X-Ray powder diffraction patterns of activated **IFMC-15** (red), as-synthesized **IFMC-15** (blue) and simulated **IFMC-15** (black).

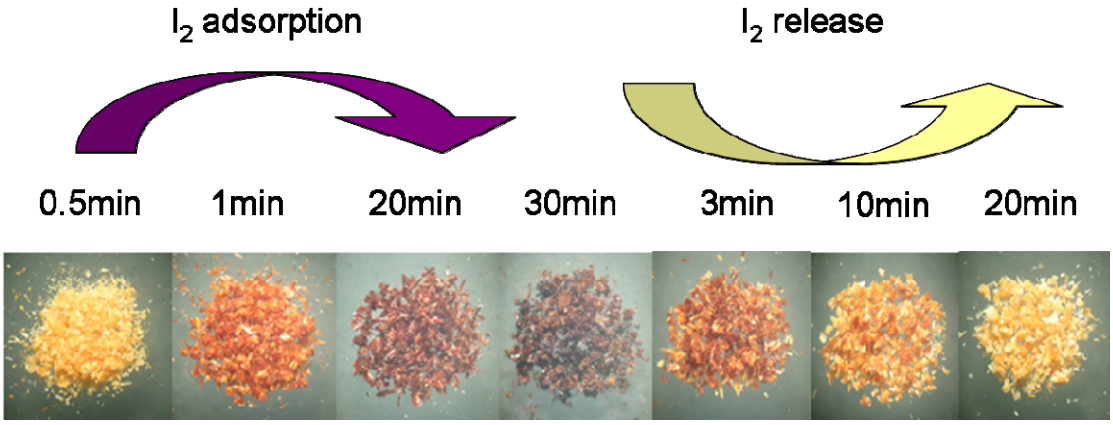

Fig. S8 The photographs for **IFMC-15** of adsorption (hexane) and releasing I_2 (ethanol).

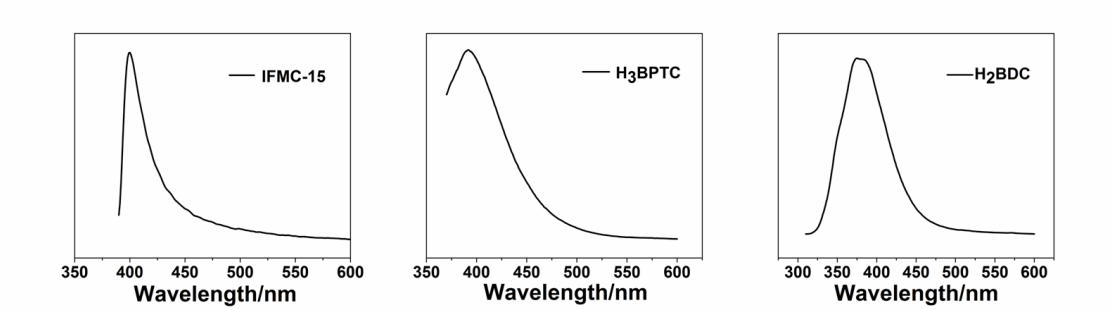

Fig. S9 Fluorescence emission spectra of **IFMC-15**, H_3BPTC ligand and H_2BDC ligand. The fluorescence emission of **IFMC-15** may be contribute to $\pi \rightarrow \pi^*$ transition of H_3BPTC ligands.

Table S2 Comparison of the I_2 content in selected iodine inclusion MOFs.[a]

MOF[b]	I_2 content wt%	Reference
$[NH_2(CH_3)_2]\cdot[Zn_4O(BPTC)_2(BDC)_{0.5}]\cdot 4.2I_2$	52.36	This work
$[Ni_2(C_{26}H_{52}N_{10})]_3[BTC]_4\cdot(I_3)_4\cdot 5I_2$ (BOF-1)	50.91	1
$[Zn(C_8H_{10}N_4)]\cdot 0.9I_2$ (ZIF-8)	50.16	2
$[Zn_3(DL\text{-lac})_2(pybz)_2]\cdot 3I_2$	49.76	3
$[Cu_6(pybz)_8(OH)_2]\cdot I_5^-\cdot I_7^-$	43.24	4
$Fe_3(HCOO)_6(I_2)_{0.84}$	32.76	5
$[Cd(L^1)_2(ClO_4)_2]\cdot 2I_2$	31.74	6
$[Cu_2(bitmb)_2Cl_4]\cdot I_2$	23.43	7
$[Zn(C_6H_8O_8)]\cdot 0.3I_2$	21.78	8
$[Zn_7(L^2)_3]\cdot[Zn_5(L^2)_3]\cdot 2.65I_2$	13.80	9
$[Cu(L^3)_2(H_2O)_{0.5}](NO_3)_{1.16}(I^-)_{0.84}$	9.55	10
$[Zn_2(L^4)(H_2O)_2]\cdot(NO_3)\cdot 0.25I_2$	5.93	11

[a] In order to compare I_2 sorption capacity of these compounds on the same level, all the wt% values of these compounds are calculated directly from the solvent excluded formulas given above.

[b] H_3BPTC = biphenyl-3,4,5-tricarboxylate; H_2BDC = 1,4-benzenedicarboxylate; Na_3BTC = 1,3,5-benzenetricarboxylate; *DL*-lac = DL-lactate; pybz =4-pyridylbenzoate; L^1 = 4-amino-3,5-bis(4-pyridyl-3-phenyl)-1,2,4-triazole;

bitmb = 1,3-bis(imidazol-1-ylmethyl)-2,4,6-trimethylbenzene;

L^2 = N-phenyl-N0-phenylbicyclo[2,2,2]oct-7-ene-2,3,5,6-tetracarboxdiimide tetracarboxylic acid;

L^3= 4-(9,9-dibutyl-7-(pyridin-4-yl)-9H-fluoren-2-yl)pyridine;

L^4 = triethyl 4',4'',4'''-(2,4,6-trimethylbenzene-1,3,5-triyl)tris(methylene)tribiphenyl-4-carboxylate.

1 H. J. Choi and M. P. Suh, *J. Am. Chem. Soc.,* 2004, **126**, 15844.

2 D. F. Sava, M. A. Rodriguez, K. W. Chapman, P. J. Chupas, J. A. Greathouse, P. S. Crozier and T. M. Nenoff, *J. Am. Chem. Soc.,* 2011, **133**, 12398.

3 M.-H. Zeng, Q.-X. Wang, Y.-X. Tan, S. Hu, H.-X. Zhao, L.-S. Long and M. Kurmoo, *J. Am. Chem. Soc.,* 2010, **132**, 2561.

4 Z. Yin, Q.-X. Wang and M.-H. Zeng, *J. Am. Chem. Soc.,* 2012, **134**, 4857.

5 Z. M. Wang, Y. J. Zhang, T. Liu, M. Kurmoo and S. Gao, *Advanced Functional Materials,* 2007, **17**, 1523.

6 Q.-K. Liu, J.-P. Ma and Y.-B. Dong, *Chem. Commun.,* 2011, **47**, 7185.

7 L. Dobrzańska, G. O. Lloyd, H. G. Raubenheimer and L. J. Barbour, *J. Am. Chem. Soc.,* 2005, **128**, 698.

8 B. F. Abrahams, M. Moylan, S. D. Orchard and R. Robson, *Angew. Chem. Int. Ed.,* 2003, **42**, 1848.

9 Z.-J. Zhang, W. Shi, Z. Niu, H.-H. Li, B. Zhao, P. Cheng, D.-Z. Liao and S.-P. Yan, *Chem. Commun.,* 2011, **47**, 6425.

10 J.-P. Ma, Y. Yu and Y.-B. Dong, *Chem. Commun.,* 2012, **48**, 2946.

11 L. Chen, K. Tan, Y.-Q. Lan, S.-L. Li, K.-Z. Shao and Z.-M. Su, *Chem. Commun.,* 2012, **48**, 5919.

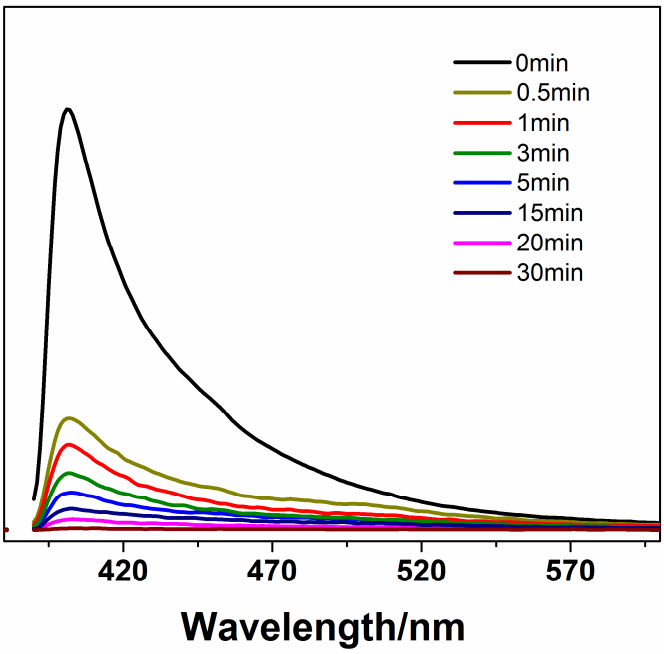

(a)

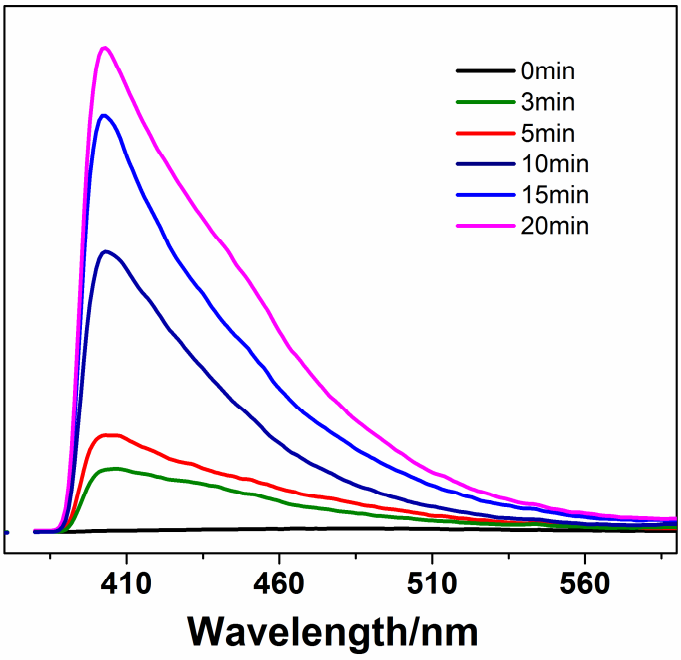

(b)

Fig. S10 (a) Photoinduced solid state emission spectra of **IFMC-15**, its I_2-loaded samples luminescence change at 0~30 min (λex = 321 nm and λem = 405 nm). After 30 min, the emission spectra of the resulted crystalline solids did not appear to change with time, indicating that the guest exchange of I_2 was basically in equilibrium. (b) After immersed in ethanol for 20 min, the luminescence intensity of **IFMC-15** was gradually recovered.

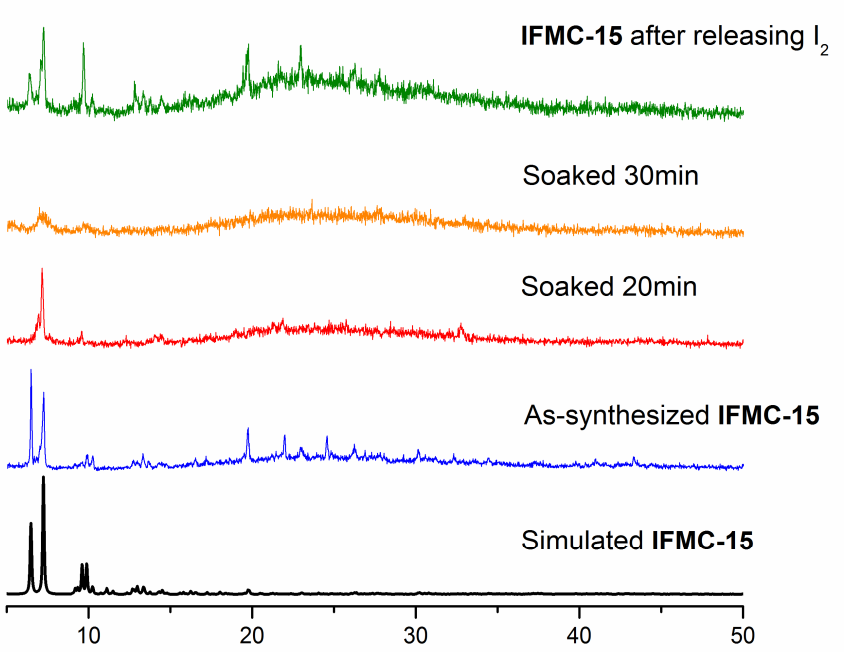

Fig. S11 X-Ray powder diffraction patterns of **IFMC-15** after releasing I_2 (green), **IFMC-15** soaked in a hexane solution (0.03 mol·L^{-1}) of I_2 at room temperature for 30 minutes (yellow), 20 minutes (red), as-synthesized **IFMC-15** (blue) and simulated **IFMC-15** (black)

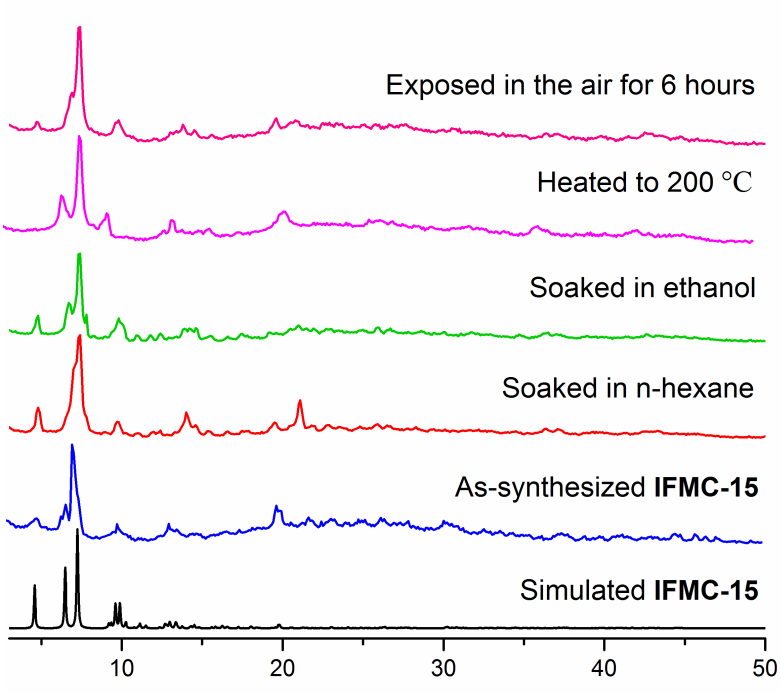

Fig. S12 PXRD patterns of **IFMC-15** exposed in the air for 6 hours (pink), heated to 200 °C for 1 hour (purple), immersed in ethanol (green), immersed in n-hexane (red), as-synthesized **IFMC-15** (blue) and simulated **IFMC-15** (black).

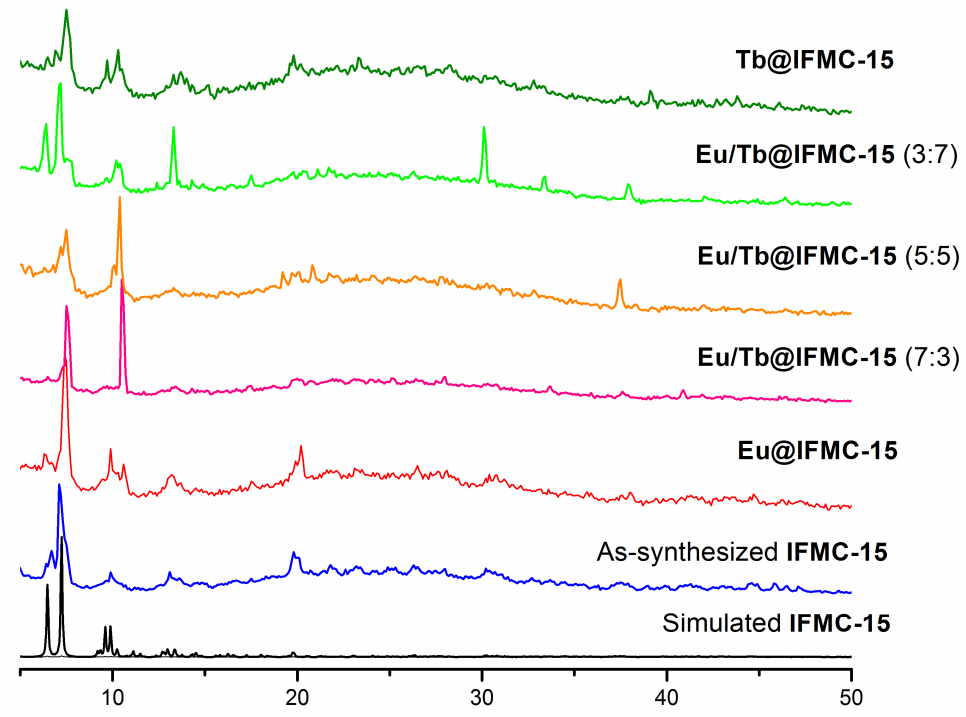

Fig. S13 X-Ray powder diffraction patterns of **Tb@IFMC-15** (green), **Eu/Tb@IFMC-15** with different proportions, **Eu@IFMC-15** (red), as-synthesized **IFMC-15** (blue) and simulated **IFMC-15** (black).

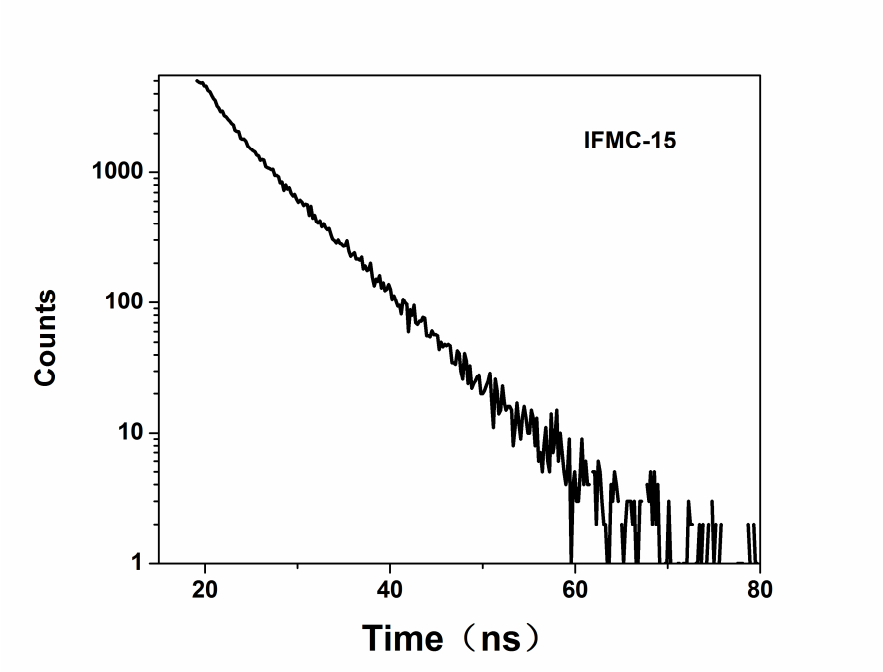

(a)

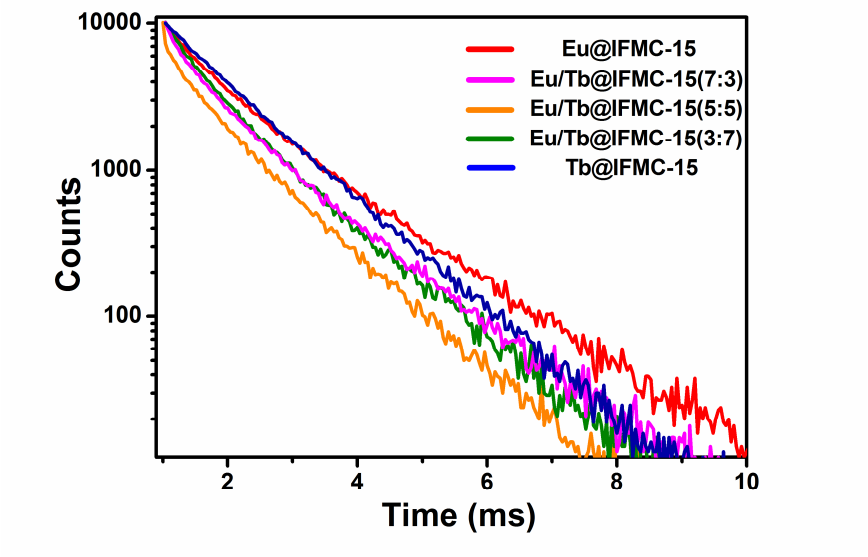

(b)

Fig. S14 Luminescence decay curves for (a) compound **IFMC-15**, (b) **Eu@IFMC-15**, **Eu/Tb@IFMC-15** (7:3), **Eu/Tb@IFMC-15** (5:5), **Eu/Tb@IFMC-15** (3:7) and **Tb@IFMC-15**. The results are 1.37, 1.19, 1.02, 1.12 and 1.13 ms respectively, while the pure MOF sample is 5.81 ns.

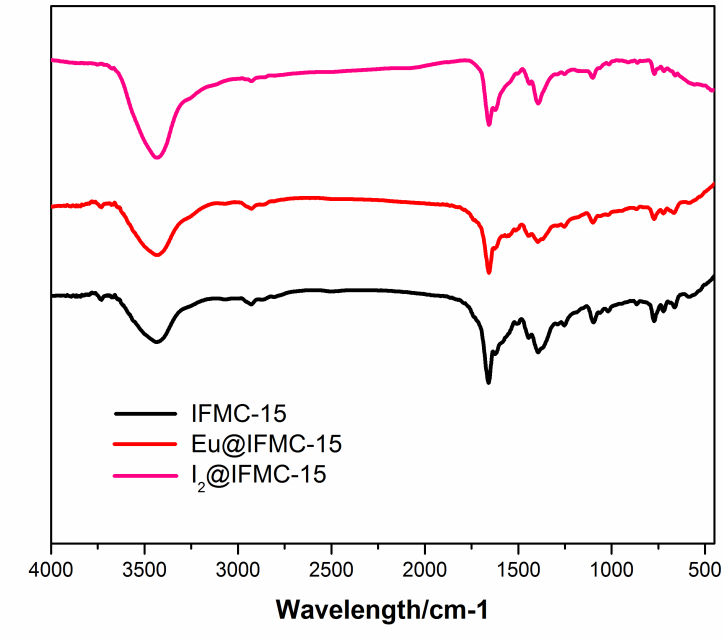

Fig. S15 FT-IR spectra of fresh **IFMC-15** and the samples of Eu^{3+} adsorption and I_2 adsorption at room temperature.

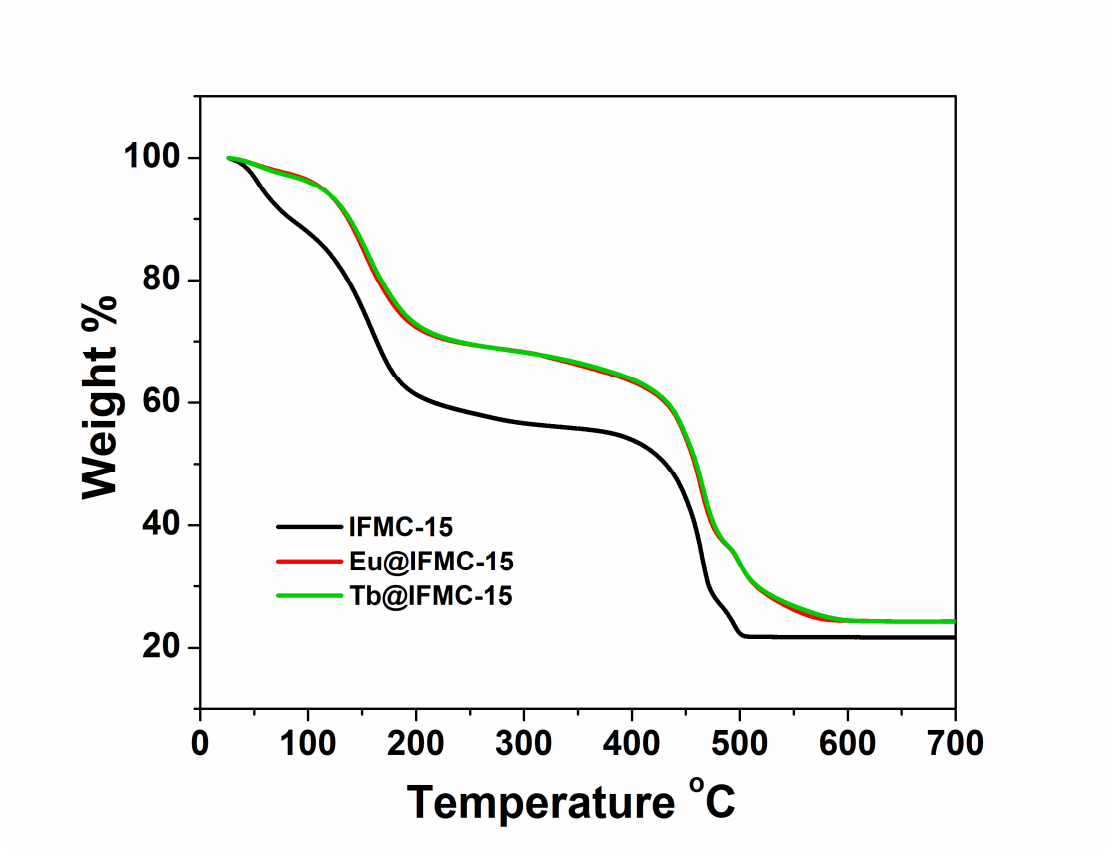

(a)

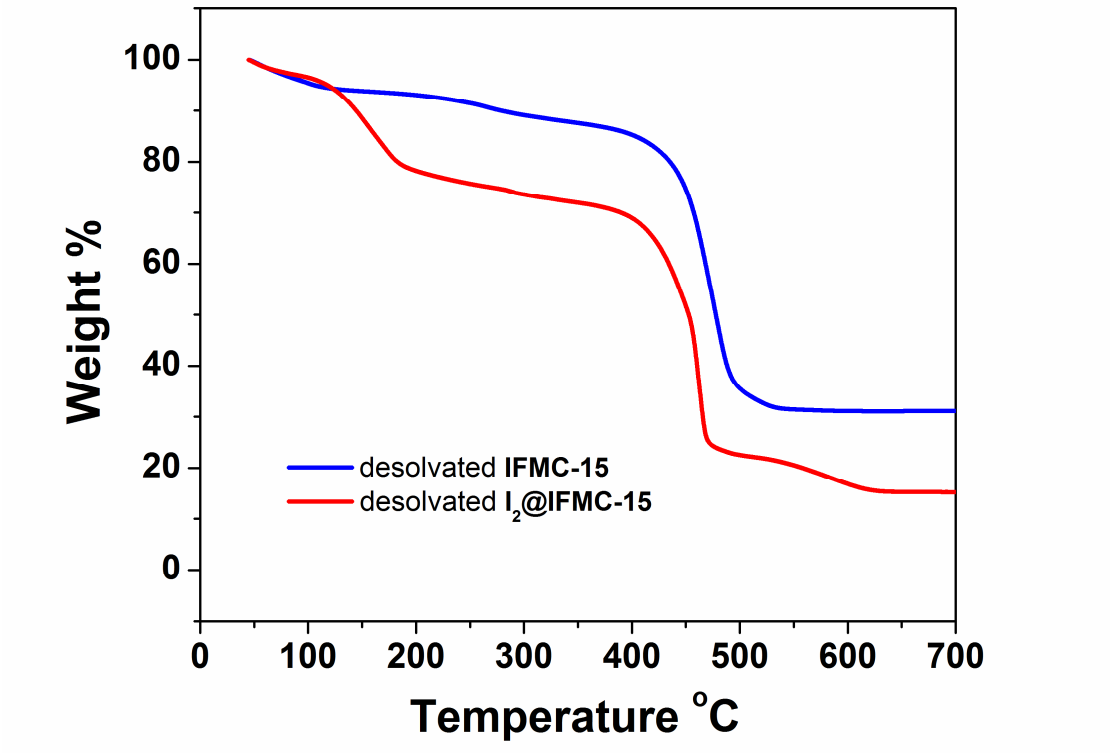

(b)

Fig. S16 TGA curves of (a) **IFMC-15** (black)**, Eu@IFMC-15** (red), **Tb@IFMC-15** (green)(**IFMC-15** immersed in a DMF solution of Ln^{3+} (0.24 mol/L) for 60 hours); (b) **IFMC-15** (blue, solvent was removed after soaking **IFMC-15** in hexane) and **I_2@IFMC-15** (red, solvent was removed after immersing **IFMC-15** in a hexane solution of I_2 (0.03 mol/L) for 12 hours) respectively. For Fig. S16 (a) the weight loss for **IFMC-15, Eu@IFMC-15**, and **Tb@IFMC-15** at about 120 °C is corresponded to the loss of the solvent, for Fig. S16 (a) and (b), the weight loss at about 440 °C is corresponded to the collapse of the whole framework, and for Fig. S16 (b), the weight loss between 200 °C to 400 °C is corresponded to the loss of iodine on the surface and in the framework.

Table S3. ICP analysis for **I_2@IFMC-15**

I_2@IFMC-15	**Concentration (ppm)**	**wt%**	**Molar (10^{-3} mol/L)**
Zn	108.5	13.04	1.66
I	440.0	52.86	3.46
I_2 : Zn	2.03 : 1	2.03 : 1	1.04 : 1

Table S4. ICP analysis for **Eu@IFMC-15, Eu/Tb@IFMC-15** (5:5) and **Tb@IFMC-15.**

Eu@IFMC-15	**Concentration (ppm)**	**wt%**	**Molar (10^{-3} mol/L)**
Zn	143.00	17.88	2.18
Eu	25.35	3.17	0.16
Eu : Zn	0.18 : 1	0.18 : 1	0.07 : 1

Eu/Tb@IFMC-15 (5:5)	**Concentration (ppm)**	**wt%**	**Molar (10^{-3} mol/L)**
Zn	141.44	17.68	2.16
Eu/Tb	12.72/12.56	1.59/1.57	0.08/0.08
Eu : Tb : Zn	0.09 : 0.09 : 1	0.09 : 0.09 : 1	0.04 : 0.04 : 1

Tb@IFMC-15	**Concentration (ppm)**	**wt%**	**Molar (10^{-3} mol/L)**
Zn	142.24	17.78	2.17
Tb	24.72	3.09	0.16
Tb : Zn	0.17 : 1	0.17 : 1	0.07 : 1

ICP analysis shows that each unit cell in **IFMC-15** can accommodate about 16.71 I_2 molecules or 1.22 Ln^{3+} ions according to the Mol ratios of Ln/Zn and I_2/Zn.

wt% results based on ICP analysis:

First, we weigh a certain quantity of the crystal (**I_2@IFMC-15** or **Ln@IFMC-15**) accurately (m);

Second, we dissolve the sample into the HNO_3 aqueous solution (1:1) and fix the volume to 25 ml;

Thirdly, we test every component concentration in the solution by ICP analysis and the data given by the instrument is the concentration (C, ppm), as shown in the second column in table S3 and table S4;

Finally we get the wt% (I, Ln and Zn) by the calculation method given below:

$$\text{wt \%} = \frac{C * 25 * 10^{-6}}{m} * 100\ \%$$

And these results are also supported by the thermal gravimetric analysis.

S4. Electrical conductivity values (σ) of IFMC-15 and I_2@IFMC-15

A bulk sample of colorless crystals of **IFMC-15** were washed twice with anhydrous DMF (2×10 mL)-each time after the mother liquid (of DMF) was decanted, the crystals were allowed to soak for 6 h before the DMF was decanted. The crystals were then similarly washed three times with dichloromethane (3×10 mL)—again, the

crystals were soaked for 12 hours before the dichloromethane was decanted. After the final dichloromethane wash, the solvent was decanted and the resultant crystals were evacuated with an oil pump at 40 °C for 30 minutes to give 0.98 g of **IFMC-15**. Half of the activated **IFMC-15** were soaked in the hexane solution of I_2 (0.03 mol/L) for 12 hours, and then were evacuated with an oil pump at 40 °C for 30 minutes to give 0.489 g of activated **I_2@IFMC-15**. All of the activated **IFMC-15** and **I_2@IFMC-15** were crushed to powder and pressed into a 1 mm thickness film respectively. The accurate thickness is measured with a screw micrometer and the results are 0.895 mm and 0.990 mm separately. Square resistances are 10.8 MΩ for **I_2@IFMC-15** and 951.5 MΩ for **IFMC-15**. Converted into electrical conductivity, the values (σ) are 2.07×10^{-7} S/cm for **I_2@IFMC-15** which is in the semiconductor range and 2.59×10^{-9} S/cm for **IFMC-15**.